# A High-Performance $Hg^+$ Trapped Ion Frequency Standard

J. D. Prestage, R. L. Tjoelker, G. J. Dick, and L. Maleki
Communications Systems Research

*A high-performance frequency standard based on $^{199}Hg^+$ ions confined in a hybrid RF/dc linear ion trap has been demonstrated. This trap permits storage of large numbers of ions with reduced susceptibility to the second-order Doppler effect caused by the RF confining fields. A 160-mHz-wide atomic resonance line for the 40.5-GHz clock transition is used to steer the output of a 5-MHz crystal oscillator to obtain a stability of $2 \times 10^{-15}$ for 24,000-second averaging times. Measurements with a 37-mHz line width for the $Hg^+$ clock transition demonstrate that the inherent stability for this frequency standard is better than $1 \times 10^{-15}$ at 10,000-second averaging times.*

## I. Introduction

Atomic frequency standards with high stability for averaging times $\tau$ longer than 1000 seconds are necessary for a variety of astrophysical measurements and long baseline spacecraft ranging experiments. The millisecond pulsar, PSR 1937+21, shows stability in its rotational period that exceeds that of all man-made clocks for averaging times longer than 6 months. Comparison of this pulsar period with an Earth-based clock of stability $1 \times 10^{-15}$ over averaging periods of one year may show the effects of very low frequency ($\approx$ 1 cycle per year) gravitational waves [1,2]. Spacecraft ranging measurements across the solar system would be improved with clocks whose stabilities exceed $1 \times 10^{-15}$ for averaging times of $10^4$ to $10^5$ seconds. This clock performance would also improve gravitational wave searches using spacecraft ranging data. Another use of clocks with long-term stability in NASA's Deep Space Network would be maintaining synchronization with Coordinated Universal Time (UTC).

The performance of microwave frequency standards in use today is summarized in Fig. 1 [2,3]. For short-term stability ($\tau < 150$ seconds) the JPL Superconducting Cavity Maser Oscillator (SCMO) shows stability as good as $2 \times 10^{-15}$ for averaging times extending to 2000 seconds [4].[1] Hydrogen masers are presently the most stable frequency standard for $150 < \tau < 30{,}000$ seconds and are the primary standards in use at each Deep Space Communications Complex. For averaging times greater than 6 months the millisecond pulsar PSR 1937 + 21 exceeds the stability of international timekeeping abilities at a level of 1 to 2 parts in $10^{-14}$ [3]. For $\tau > 10^6$ seconds the most stable clock yet measured is the $Hg^+$ ion standard based on $2 \times 10^6$ ions confined in an RF Paul trap [2,5]. The subject of the present article is a linear ion trap (LIT) based $Hg^+$ frequency standard now being tested at the Frequency Standards Laboratory (FSL) at JPL. Stability measurements of the $Hg^+$ standard using an H-maser local oscillator are shown in Fig. 1. Determination of the long-term stability ($\tau > 10{,}000$ seconds) is limited by instabilities in available reference H-masers.

[1] R. T. Wang, private communication, Jet Propulsion Laboratory, Pasadena, California, July 1991.

Typically the largest source of frequency offset in standards based on ions confined in Paul traps stems from the motion of the ions caused by the trapping fields via the second-order Doppler or relativistic time dilation effect. Though increasing ion number will lead to an increasing signal to noise ratio in the measurement of the clock transition, the frequency offset also grows with the number of ions forcing a trade-off situation. Often fewer ions are trapped in order to reduce the (relatively) large offset and frequency instabilities which may result.

## II. Linear Ion Trap

In a conventional hyperbolic Paul trap, ions are trapped around a node of the RF electric field at the center. The strength of the electric field and the resulting micromotion of the trapped particles grows linearly with distance from this node point. As ions are added the size of the ion cloud grows until the second-order Doppler shift arising from the micromotion in the trapping field dominates the second-order Doppler shift from the ion's thermal motion at room temperature. For typical operating conditions [6] a spherical cloud containing $2 \times 10^6$ mercury ions shows a second-order Doppler shift of $2 \times 10^{-12}$, a value some 10 times larger than that due to thermal motion alone. In order to increase the number of stored ions with no corresponding increase in second-order Doppler shift from ion micromotion, a hybrid RF/dc LIT [7] was proposed[2] and developed. This trap confines ions along a line of nodes of the RF field effectively providing the same capability as a large number of hyperbolic traps together. The trapping force transverse to the line of nodes is generated by the ponderomotive force as in conventional Paul traps while the axial trapping force is provided by dc electric fields [7–10]. Unlike conventional RF traps this linear trap will hold positive or negative ions but not both simultaneously. A related trap using purely ponderomotive forces to confine charged particles is the racetrack trap [11,12].

The second-order Doppler shifts, $\Delta f/f$, generated by the trapping fields for a cloud of ions in these two types of traps can be compared, assuming that both traps are operated with the same RF trapping force as that characterized by the ion secular frequency $\omega$. If the same number of ions $N$ is held in both traps, the average distance from an ion to the node of the trapping field is greatly reduced in the linear trap. Since the distance from the node determines the magnitude of the RF trapping field, the second-order Doppler shift of an ion's clock frequency due to motion in the trapping field is reduced from that of a hyperbolic trap. If $R_{sph}$ is the ion cloud radius in the hyperbolic trap and $L$ is the ion cloud length in the linear trap, the Doppler shift in the two traps is related by [7]

$$\left(\frac{\Delta f}{f}\right)_{lin} = \frac{5}{3}\frac{R_{sph}}{L}\left(\frac{\Delta f}{f}\right)_{sph} \tag{1}$$

As more ions are added to the linear trap this shift will increase. It will equal that of the spherical ion cloud in a hyperbolic trap when

$$N_{lin} = \frac{3}{5}\frac{L}{R_{sph}}N_{sph} \tag{2}$$

Equations (1) and (2) are valid when the ion cloud radii, $R_{lin}$ and $R_{sph}$, are much larger than the Debye length, which is the characteristic plasma density decay length at the ion cloud edge and is about 0.4 mm for typical $Hg^+$ ion plasmas used in frequency standard work [6].

In addition to its larger ion storage capacity, the dependence of the second-order Doppler shift on trapping parameters in a linear trap is very different from that in a conventional Paul trap. For many ions in a Paul trap this shift is given by [6,7]

$$\left(\frac{\Delta f}{f}\right)_{sph} = -\frac{3}{10c^2}\left(\frac{N\omega q^2}{4\pi\epsilon_o m}\right)^{2/3} \tag{3}$$

where $\omega$ is the secular frequency for a spherical ion cloud containing $N$ ions each with charge to mass ratio $q/m$, $c$ is the speed of light, and $\epsilon_o$ is the permittivity of free space. Ions in a long linear trap where end effects are negligible show a second-order Doppler shift from the motion generated by the RF confining field given by [7]

$$\left(\frac{\Delta f}{f}\right)_{lin} = -\left(\frac{q^2}{8\pi\epsilon_o mc^2}\right)\frac{N}{L} \tag{4}$$

where $N/L$ is the linear number density of ions in the trap.

In contrast to the spherical case described in Eq. (3), this expression contains no dependence on trapping field strength, as characterized by $\omega$, and depends only on the linear ion density $N/L$. If for example, the RF confining voltage increases and consequently the micromotion at a given point in space increases, the ion cloud radius will

[2] J. D. Prestage, *OSTDS Advanced Systems Review*, DSN RTOP 310-10-62 (internal document), Jet Propulsion Laboratory, Pasadena, California, pp. 64–68, June 14–15, 1988.

decrease so that the second-order Doppler shift (averaged over the cloud) from ion micromotion remains constant. Similar statements can be made about variations in any parameter that affects the radial confinement strength [8].

The sensitivity of the finite length linear trap to variations in radial trapping strength (characterized by $\omega$) is [8]

$$\frac{\delta\left(\frac{\Delta f}{f}\right)_{lin}}{\left(\frac{\Delta f}{f}\right)_{lin}} = -2\frac{R_t}{L}\frac{\delta\omega}{\omega} \tag{5}$$

and to variations in endcap voltage is

$$\frac{\delta\left(\frac{\Delta f}{f}\right)_{lin}}{\left(\frac{\Delta f}{f}\right)_{lin}} = 2 \cdot \frac{R_t}{L}\frac{\delta V_e}{V_e} \tag{6}$$

where $R_t$ is the trap radius. The Paul trap shows a corresponding sensitivity to trapping field strength variations of

$$\frac{\delta\left(\frac{\Delta f}{f}\right)_{sph}}{\left(\frac{\Delta f}{f}\right)_{sph}} = -\frac{2}{3}\frac{\delta\omega}{\omega} \tag{7}$$

A comparison of Eqs. (5) and (7) shows the linear trap based frequency standard to be less sensitive to variations in trapping field strength than the Paul trap by a factor of $3R_t/L$. For the trap described in the next section this factor is about 1/3.

## III. Operation With H-Maser Local Oscillator

Ions are produced inside the linear trap (Fig. 2) by an electron pulse along the trap axis which ionizes a neutral background vapor of $^{199}$Hg. A helium buffer gas ($10^{-5}$ mbar) collisionally cools the ions to near room temperature. Resonance radiation (194 nm) from a $^{202}$Hg discharge lamp optically pumps the ions into the $F = 0$ hyperfine level of the ground state [13]. This UV light is focused onto the central 1/3 of the 75-mm-long ion cloud. The thermal motion of the ions along the length of the trap will carry all the ions through the light field so that pumping is complete in about 1.5 seconds for typical lamp intensities.

To minimize stray light entering the fluorescence collection system this state selection light is collected in a pyrex horn as shown in Fig. 2. The location of the $LaB_6$ electron filament is also chosen to prevent light from entering the collection system. The filament's placement and relatively cool operating temperature, together with effective filtering of the state selection/interrogation UV light in the input optical system, allow frequency standard operation without the use of a 194-nm optical bandpass filter in the collection arm. This triples data collection rates since such filters typically have about 30-percent transmission for 194-nm light.

Microwave radiation (40.5 GHz), multiplied from an appropriate local oscillator (LO), passes through the trap perpendicular to the trap axis satisfying the Lamb-Dicke requirement that the spatial extent of the ion's motion along the direction of propagation of the microwave radiation be less than a wavelength. The microwaves enter through the pyrex horn (see Fig. 2) in opposition to the UV state selection/interrogation light. This allows collection of atomic fluorescence in both directions perpendicular to the incident pumping light. For the resonance and stability data shown in this article, fluorescence was collected in only one of these two directions.

The technique of successive oscillatory fields [14] has been used to probe the approximately 40.5-GHz hyperfine clock transition in $^{199}Hg^+$ ions confined to the linear trap. In the initial measurements the 40.5-GHz signal is derived from an active hydrogen maser frequency source as shown in Fig. 3. A representative resonance line of the $^{199}Hg^+$ clock transition is shown in Fig. 4. State selection and interrogation is accomplished during the 1.5 seconds following the lamp turn-on. It is necessary to switch the UV state selection/interrogation light level to near zero during the microwave interrogation period to prevent light shifts and broadening of the clock transition. A background light level of about 300,000 counts per 1.5-sec collection period has been subtracted to generate the resonance shown. The successive oscillatory field pulses consist of two 0.35-sec microwave pulses separated by a 2.5-sec free precession period. The data shown in Fig. 4 are averages of 10 scans with a 10-mHz frequency step size.

The central portion of the narrowest resonance lines yet obtained with this apparatus is shown in Fig. 5. This line is derived from two 0.275-second pulses separated by a 16.5-second free precession period [15]. The line width of 30 mHz represents a line $Q$ of over $1 \times 10^{12}$ on the 40.5-GHz transition. The data displayed are an average of four full scans and represent the highest $Q$ transition ever measured in a microwave atomic transition.

To determine the frequency stability of the overall system of ions, trap, and microwave source, the output fre-

quency of the 40.5-GHz source has been locked to the central peak of the 160-mHz resonance in a sequence of 16,384 frequency measurements. The time required for each measurement is about 7 seconds and the loop response time was five measurement cycles. By averaging the frequencies of $2^N$ adjacent measurements ($N = 1, 2, \cdots, 13$), the Allan deviation is formed as shown in Fig. 6(a). Performance of the linear ion trap based $Hg^+$ standard measured in this manner is $2 \times 10^{-13}/\sqrt{\tau}$ for averaging times $\tau \leq 20,000$ seconds, beyond which H-maser frequency instabilities limit the measurement. Figure 6(b) shows better performance obtained with a 37-mHz-wide resonance generated by two 0.35-second $\pi/2$ pulses with a 13-second precession period between. The stability measured in this mode of operation is $1 \times 10^{-15}$ for an averaging time of 10,000 seconds.

At present no thermal regulation is incorporated into the ion standard itself. However, for all stability measurements described the ion trap standard together with its support electronics were housed in an environmentally controlled test chamber where temperature variations were regulated to approximately ± 0.05 deg C. Environmental sensitivities, leading perturbations, and control constraints of the $Hg^+$ trapped ion frequency standard are described and quantified in reference [19].

## IV. Operation With a Crystal Oscillator

In this section is described the long-term stability achieved when a commercial (Oscilloquartz 8600B no. 104) 5-MHz quartz crystal oscillator of superior performance is servoed to the 160-mHz $Hg^+$ ion resonance as shown in Fig. 4. The schematic of this system is shown in Fig. 7. A frequency stability measurement of the $Hg^+$ steered crystal using two H-masers in the measurement system (designated Deep Space Network (DSN) 2 and DSN3) as references has been carried out using the JPL Frequency Standards Lab (FSL) measurement system.

The results of this 63-hour comparison are shown in Figs. 8(a) and (b). The first figure shows the Allan deviation of the $Hg^+$ steered crystal as measured against DSN2 (upper trace) and against DSN3 (lower trace). For averaging times less than 10 seconds the Allan deviation is that of the unsteered crystal oscillator since the loop attack time is about 10 seconds. For averaging times shorter than about 13,000 seconds the $Hg^+$ standard shows the same stability independent of a reference maser. For $\tau > 20,000$ seconds the Allan deviation of the $Hg^+$ versus DSN2 is the same as that for DSN2 versus DSN3 [see Fig. 8(b)] indicating that DSN2 has the limiting performance of the three standards under test for this averaging time period. The lower trace of Fig. 8(a) shows a $Hg^+$ standard stability of $2 \times 10^{-15}$ for $\tau = 24,000$ seconds beyond which instabilities in DSN3 probably limit the measurement. A second $Hg^+$ ion standard is now under construction, which will enable stability measurements beyond 24,000 seconds.

## V. Local Oscillator Considerations

Fluctuations in the local oscillator (LO) limit performance of a trapped ion standard in two ways. As discussed above, slow variations of the crystal LO are compensated by action of the servo system. The effectiveness of this compensation increases with the measuring time, so that for longer measuring times performance approaches the $1/\sqrt{\tau}$ dependence which is characteristic of passive standards. This behavior is clearly shown in Fig. 8(a).

However, fast fluctuations in the LO also degrade performance of the standard by an effect that adds to the (white) fluctuation of the photon count from measurement to measurement [16–18]. This limitation continues to the longest times, having the same $1/\sqrt{\tau}$ dependence on measuring time $\tau$ as the inherent performance of the standard itself. The cause of this effect can be traced to a time varying sensitivity to LO frequency which is inherent in the interrogation process. This limitation was evaluated in a recent calculation for several types of sequentially interrogated passive standards [18].

Using this same methodology, one can calculate the LO-induced performance degradation for this particular interrogation scenario. Here, two RF pulses of 0.35-second length are separated by a delay of 2.5 seconds. A dead time of 3.8 seconds follows to give the cycle time of $t_c = 7$ seconds. The authors' quartz LO shows flicker frequency noise with an approximately flat Allan deviation of $1.5 \times 10^{-13}$. For this LO a contribution was calculated to the Allan deviation of the trapped ion source of $2.6 \times 10^{-13}/\sqrt{\tau}$. This value is slightly larger than the $2.0 \times 10^{-13}/\sqrt{\tau}$ due to random fluctuations in the photon count, again based on actual operating conditions. The two contributions can be combined to give a limiting stability of $3.3 \times 10^{-13}/\sqrt{\tau}$ which is plotted along with the data in Fig. 8(a). The data confirm this analysis by a very close approach to the line for measuring times $\tau > 10^3$ seconds.

Both LO and intrinsic statistical performance limitations may be reduced by increasing the interrogation time, as long as the dead time is not increased. The implicitly higher $Q$ and reduced (relative) dead time would result in a comparable improvement for each of the two contribu-

tions. For example, an increase in the interrogation time by four times would reduce the limiting $1/\sqrt{\tau}$ Allan deviation by half.

However, it is clear that as performance improves to make possible trapped ion performance in the low $10^{-14}/\sqrt{\tau}$ range, quartz crystal LO performance will not be sufficient in itself to keep pace. In this case a cryogenic LO with $10^{-14}$ type stability for short times could be used, or a quartz LO with alternatively interrogated traps to give a uniform servo sensitivity with time [18].

## VI. Conclusions

By steering a 5-MHz crystal oscillator to a 160-mHz atomic resonance ($Q = 3.3 \times 10^{11}$), performance of $2 \times 10^{-15}$ has been measured for $\tau = 24{,}000$ seconds limited by the stability of available reference hydrogen masers. Line $Q$s as high as $1.3 \times 10^{12}$ have been measured [15], indicating consequent performance for this trap as good as $5 \times 10^{-14}/\sqrt{\tau}$ for $\tau > 150$ seconds. While using a hydrogen maser as a local oscillator an Allan deviation of $1 \times 10^{-15}$ at 10,000 seconds with a 37-mHz resonance line has been measured.

## Acknowledgments

The authors thank R. Berends for making the $^{202}$Hg lamps and W. Diener, A. Kirk and R. Taylor for assistance with the Frequency Standards Laboratory Test and Measurement System.

## References

[1] M. M. Davis, J. H. Taylor, J. M. Weisberg, and D. C. Backer, "High-Precision Timing Observations of the Millisecond Pulsar PSR1937+21," *Nature*, vol. 315, pp. 547–550, June 1985.

[2] D. W. Allan, M. A. Weiss, and T. K. Peppler, "In Search of the Best Clock," *IEEE Trans. Instrum. Meas.*, vol. 38, no. 2, pp. 624–630, April 1989.

[3] L. A. Rawley, J. H. Taylor, M. M. Davis, and D. W. Allan, "Millisecond Pulsar PSR 1937+21: A Highly Stable Clock," *Science*, vol. 238, pp. 761–765, November 1987.

[4] R. T. Wang and G. J. Dick, "Improved Performance of the Superconducting Cavity Maser at Short Measuring Times," *Proceedings of the 44th Ann. Symp. on Freq. Control*, IEEE (IEEE Cat. no. 87-654207), Piscataway, New Jersey pp. 89–93, 1990.

[5] L. S. Cutler, R. P. Giffard, P. J. Wheeler, and G. M. R. Winkler, "Initial Operational Experience with a Mercury Ion Storage Frequency Standard," *Proceedings of the 41st Ann. Symp. Freq. Control*, IEEE (IEEE Cat no. 87CH2427-3), Piscataway, New Jersey pp. 12–19, 1987.

[6] L. S. Cutler, R. P. Giffard, and M. D. McGuire, "Thermalization of $^{199}$Hg Ion Macromotion by a Light Background Gas in an RF Quadrupole Trap," *Appl. Phys. B*, vol. 36, pp. 137–142, January 1985.

[7] J. D. Prestage, G. J. Dick, and L. Maleki, "New Ion Trap for Frequency Standard Applications," *J. Appl. Phys.*, vol. 66, no. 3, pp. 1013–1017, August 1989.

[8] J. D. Prestage, G. R. Janik, G. J. Dick, and L. Maleki, "Linear Ion Trap for Second-Order Doppler Shift Reduction in Frequency Standard Applications," *IEEE Trans. Ultrason. Ferroelec. Freq. Contr.*, vol. 37, pp. 535–542, November 1990.

[9] G. R. Janik, J. D. Prestage, and L. Maleki, "Simple Analytic Potentials for Linear Ion Traps," *J. Appl. Phys.*, vol. 67, no. 10, pp. 6050–6055, May 1990.

[10] D. J. Wineland, J. C. Bergquist, J. J. Bollinger, W. M. Itano, D. J. Heinzen, S. L. Gilbert, C. H. Manney, and M. G. Raizen, "Progress at NIST Toward Absolute Frequency Standards Using Stored Ions," *IEEE Trans. Ultrason. Ferroelec. Freq. Contr.*, vol. 37, pp. 515–523, November 1990.

[11] H. G. Dehmelt, "Introduction to the Session on Trapped Ions," *Proceedings of the 4th Symp. Frequency Standards and Metrology*, New York: Springer-Verlag, p. 286, 1989.

[12] D. A. Church, "Storage Ring Ion Trap Derived from the Linear Quadrupole Radio Frequency Mass Filter," *J. Appl. Phys.*, vol. 40, no. 8, pp. 3127–3134, July 1969.

[13] F. G. Major and G. Werth, "Magnetic Hyperfine Spectrum of Isolated $^{199}Hg^{+}$ Ions," *Appl. Phys.*, vol. 15, pp. 201–208, January 1978.

[14] N. F. Ramsey, *Molecular Beams*, Oxford, England: Oxford University Press, 1956.

[15] J. D. Prestage, G. J. Dick, and L. Maleki, "Linear Ion Trap Based Atomic Frequency Standard," *IEEE Trans. Instr. Meas.*, vol. 40, pp. 132–136, April 1991.

[16] G. J. Dick, "Calculation of Trapped Ion Local Oscillator Requirements," *Proceedings of the 19th Annual Precise Time and Time Interval (PTTI) Applications and Planning Meeting*, Naval Observatory, Washington, D.C., pp. 133–146, 1988.

[17] C. Audoin, V. Candelier, and N. Dimarcq, "A Limit to the Frequency Stability of Passive Frequency Standards," *IEEE Trans. Instr. Meas.*, vol. 40, pp. 121–125, April 1991.

[18] G. J. Dick, J. D. Prestage, C. A. Greenhall, and L. Maleki, "Local Oscillator Induced Degradation of Medium-Term Stability in Passive Atomic Frequency Standards," *Proceedings of the 22nd Annual Precise Time and Time Interval (PTTI) Applications and Planning Meeting*, Naval Observatory, Washington, D.C., pp. 487–508, 1990.

[19] R. L. Tjoelker, J. D. Prestage, and L. Maleki, "Criteria for Ultra-Stable Operation of the Trapped Ion Frequency Standard," *TDA Progress Report 42-108*, vol. October–December 1991, Jet Propulsion Laboratory, Pasadena, California, pp. 19–30, February 15, 1992.

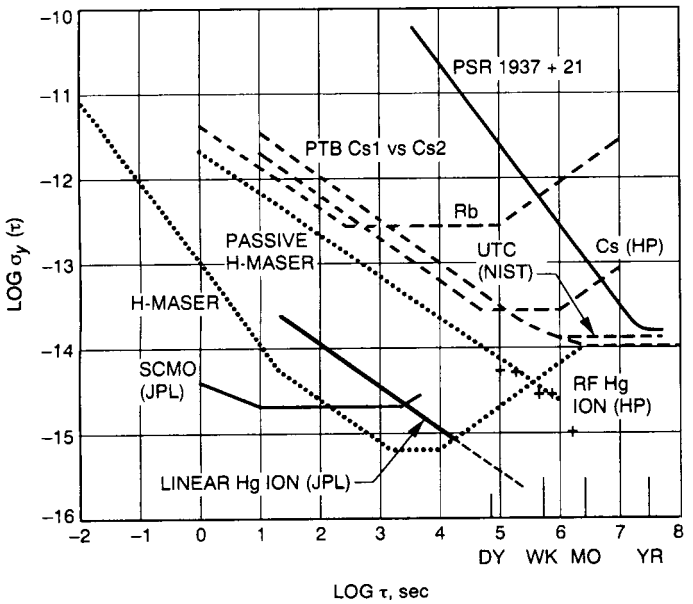


**Fig. 1. Fractional frequency stability of several precision frequency standards. (PTB = Physikalish-Technische Bundesandstalt; NIST = National Institute of Standards and Technology; HP = Hewlett Packard).**

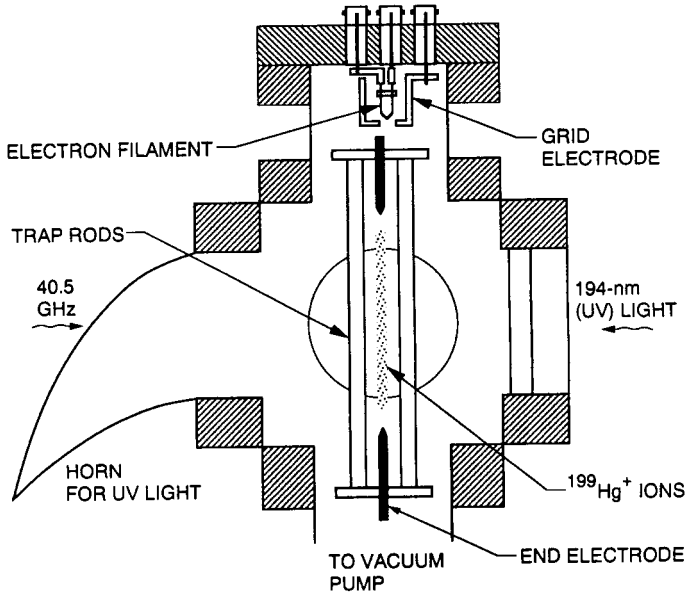


**Fig. 2. Linear ion trap assembly residing in its high vacuum enclosure. State selection light from the $^{202}Hg$ discharge lamp enters from the right, is focused onto the central 1/3 of the trap and is collected in the horn. Fluorescence from the trapped ions is collected in a direction normal to the page.**

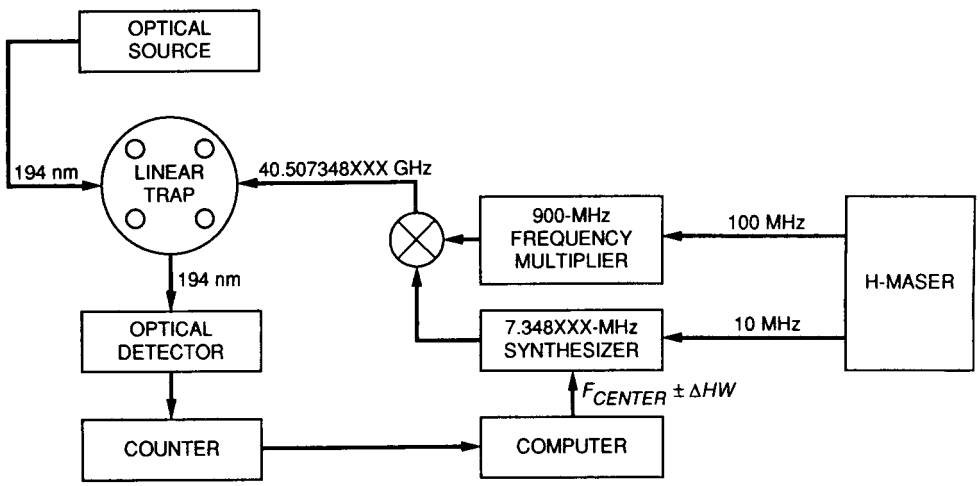


**Fig. 3. Schematic operation of the mercury ion trap using a hydrogen maser as the local oscillator.**

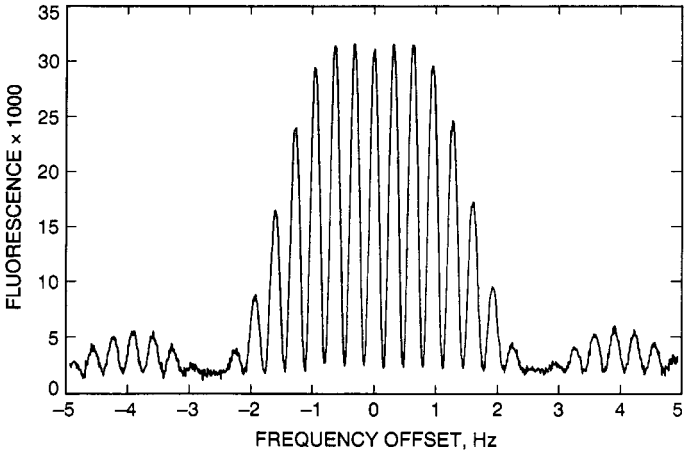


**Fig. 4. $^{199}Hg^{+}$ clock transition as measured with method of successive oscillatory fields. This line shape results from two 0.35-second microwave pulses separated by a 2.5-second free precession period. The central line is about 160 mHz wide and the data shown are an average of ten scans.**

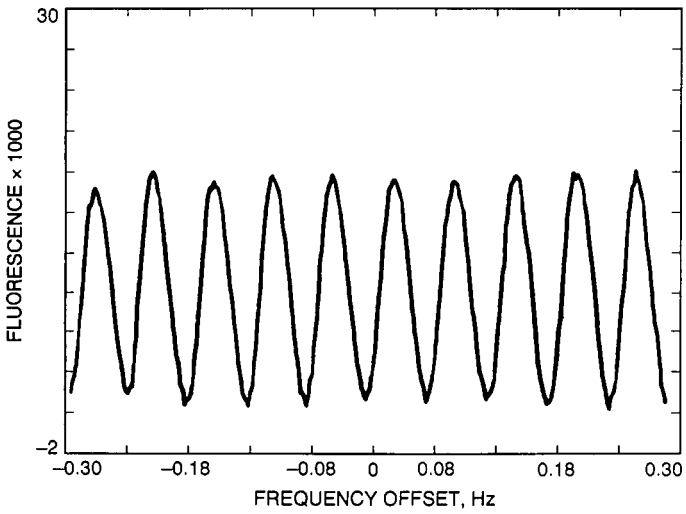


**Fig. 5. High *Q* Ramsey fringes resulting from two microwave pulses of 0.275 seconds separated by a 16-second free precession period. The fringes are about 30 mHz wide and the data shown are an average of four scans.**

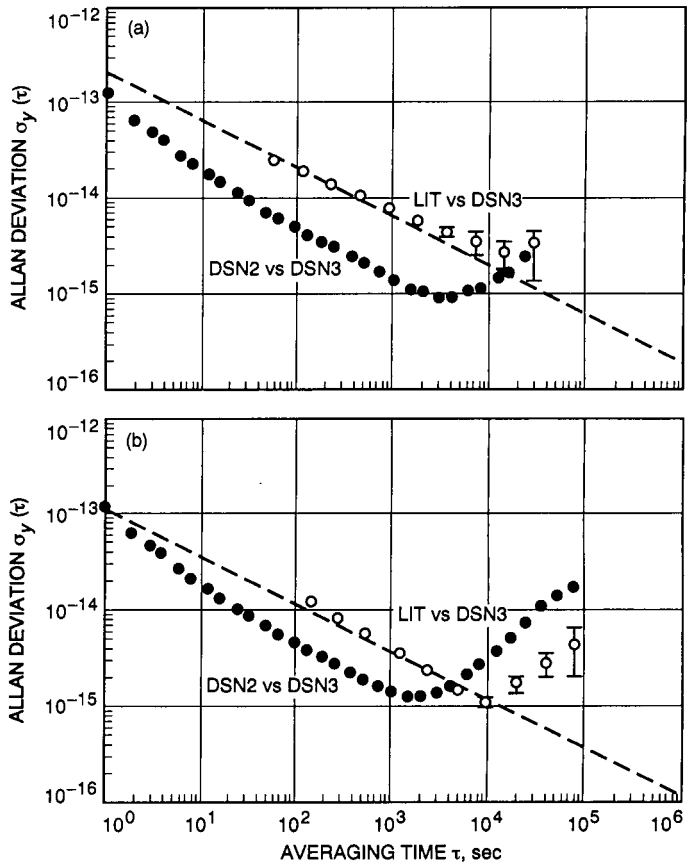


**Fig. 6. Performance of the $Hg^{+}$ system when the local oscillator is a hydrogen maser; the fractional frequency stability of the ion trap system is measured against an LO maser: (a) Stability obtained with a 160-mHz $Hg^{+}$ resonance line as shown in Fig. 4; the $2 \times 10^{-13}/\sqrt{\tau}$ line is shown for reference. (b) Stability obtained with a 37-mHz $Hg^{+}$ resonance line. Also shown is the stability comparison of the LO maser to another H-maser.**

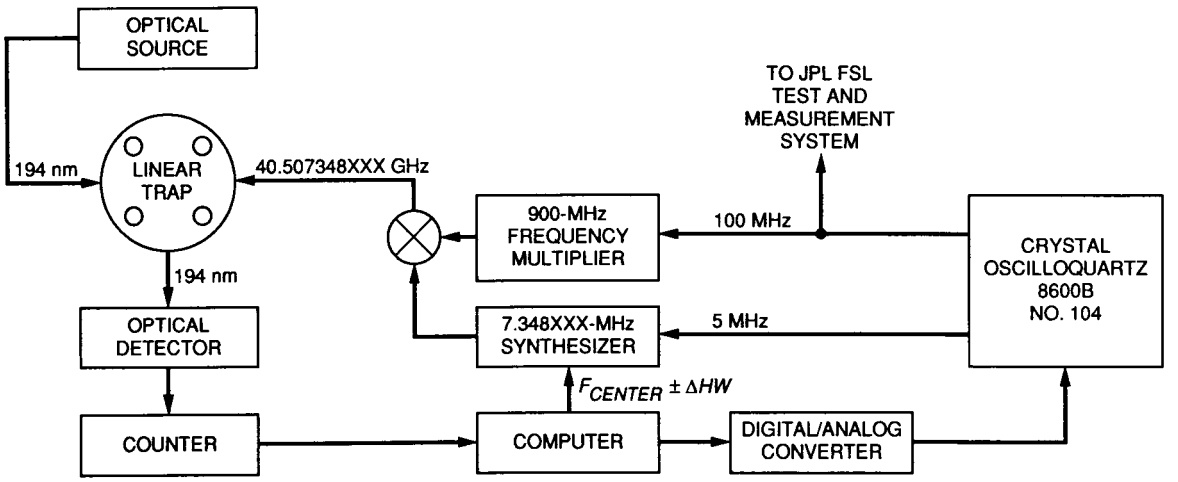


**Fig. 7. Schematic operation of the mercury ion trap to steer a quartz oscillator.**

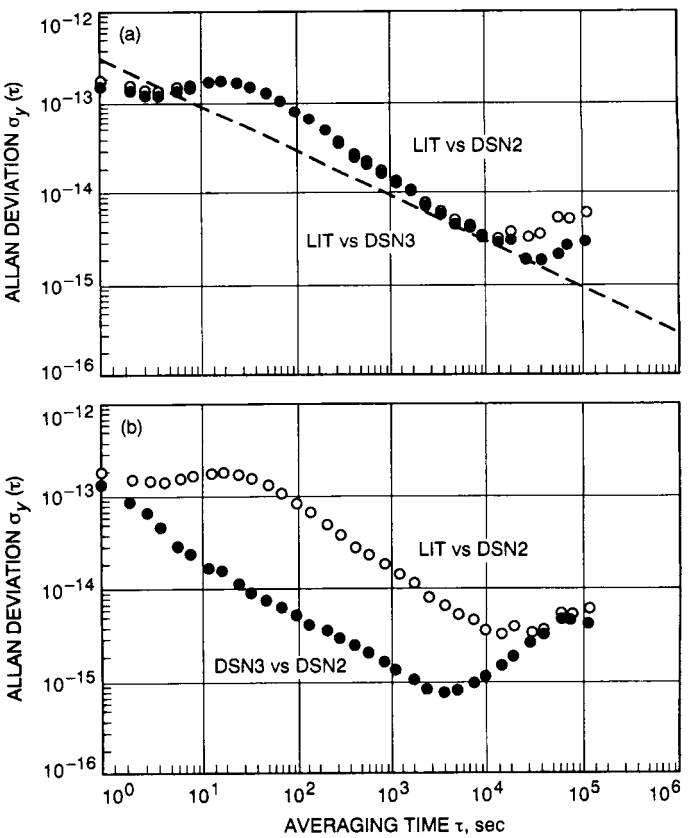


**Fig. 8. Performance of the $Hg^+$ system when the LO is a quartz oscillator: (a) the ion trap standard compared to each maser independently, distinguishing the different performance of the two masers for times $\tau \geq$ 10,000 seconds (the dashed line represents calculated $1/\sqrt{\tau}$ performance based on actual operating conditions), and (b) fractional frequency stability compared to the hydrogen maser DSN3 and maser comparison between DSN2 and DSN3.**